Morphology of renormalization-group flow for the de Almeida–Thouless–Gardner universality class

Patrick Charbonneau,[1,2] Yi Hu,[1] Archishman Raju,[3] James P. Sethna,[3] and Sho Yaida[1]
[1]*Department of Chemistry, Duke University, Durham, North Carolina 27708, USA*
[2]*Department of Physics, Duke University, Durham, North Carolina 27708, USA*
[3]*Laboratory of Atomic and Solid State Physics, Cornell University, Ithaca, New York 14853, USA*

(Received 4 August 2018; revised manuscript received 25 January 2019; published 21 February 2019)

A replica-symmetry-breaking phase transition is predicted in a host of disordered media. The criticality of the transition has, however, long been questioned below its upper critical dimension, six, due to the absence of a critical fixed point in the renormalization-group flows at one-loop order. A recent two-loop analysis revealed a possible strong-coupling fixed point, but given the uncontrolled nature of perturbative analysis in the strong-coupling regime, debate persists. Here we examine the nature of the transition as a function of spatial dimension and show that the strong-coupling fixed point can go through a Hopf bifurcation, resulting in a critical limit cycle and a concomitant discrete scale invariance. We further investigate a different renormalization scheme and argue that the basin of attraction of the strong-coupling fixed point (or limit cycle) may stay finite for all dimensions.

DOI: 10.1103/PhysRevE.99.022132

I. INTRODUCTION

Quenched disorder often leaves conspicuous marks on a system's macroscopic behavior. For instance, quenched impurities can localize excited states [1–4] and consequently turn metals into insulators with anomalous transport properties [5–7]. When coupled to an order parameter, extrinsic disorder can also destroy the would-be long-range order, altering its lower critical dimension [8]. Counterintuitively, disorder can also give rise to long-range order, albeit in the subtle, amorphous manner that breaks the permutation symmetry among fictitious replicas [9]. Although initially considered a fairly exotic proposal, this replica symmetry breaking (RSB) phenomenon has since found core applications in different fields of science [10].

The nature of the RSB phase transition, however, remains controversial. While its existence and criticality are unquestionable in a wide range of infinite-dimensional mean-field models ranging from spin to structural glasses [9–18], some have suggested that the RSB phase is completely washed out in all finite-dimensional, short-ranged models [19]. In particular the droplet-scaling scenario [20–25] proposes that there cannot be infinitely many incongruent pure states in realistic finite-dimensional models (see also Ref. [26]). Others posit that the transition survives down to the upper critical dimension, $d_{\mathrm{u}} = 6$, but disappears below it [27] (see, however, Refs. [28–30]). This second proposal is rooted in the absence of a critical fixed point in the renormalization-group (RG) flow equation at one-loop level below d_{u} [31–33]. The discovery of the Gardner transition in structural glass formers [18] has rekindled interest in this debate [33–38], and a recent two-loop RG analysis [39] (see Appendix A) challenges the above proposals by identifying a strong-coupling critical fixed point that is invisible at one-loop order, just as is the case for a class of non-Abelian gauge theories [40,41]. While the validity of the two-loop analysis in the strong-coupling regime can be questioned, it nonetheless provides a potentially viable description of the critical RSB transition in three-dimensional systems.

The difficulty associated with capturing the fate of strong-coupling fixed points through perturbative methods is well known. Even for the Ising universality class, the minimal RG equation without resummation results in the Wilson-Fisher fixed point for spatial dimensions $d = 2$ and 3 being present at one-loop, three-loop, and five-loop orders, but absent at two-loop and four-loop orders. Only after applying a certain class of resummation schemes does the existence of the fixed point become independent of loop order [42]. In the Ising case, the pre-existing experimental and theoretical evidences of criticality in two and three dimensions, together with the striking agreement of the one-loop exponents with exponents measured in three dimensions, made it clear that the qualitative change in the unresummed results was not a fundamental concern. For the critical RSB phase transition as well, a similar aggregation of evidences from theories, experiments [43–46], and simulations [47–52] will be needed to reach a steady state of understanding for the true fixed point structure. In attaining such an understanding, it is especially instructive to examine the nature of the transition as a function of d, as was instrumental for studying the Ising universality class, percolation [53,54], the glass problem [55,56], and many others [57]. Here, we thus closely analyze higher-loop RG flow equations in varying dimensions.

It is important to emphasize that the intent of the paper is not to provide a conclusive answer to the nature of the fixed point structure in finite dimensions. That answer will most likely require a concerted and sustained effort in developing various theoretical machineries, such as higher-loop calculations [58] with sophisticated resummation schemes [59,60], nonperturbative RG [61–66] (see also Appendix B), and conformal bootstrap [67–70], as well as experiments and simulations. Instead, our intent here is to suggest a few viable

physical scenarios that have heretofore been missed within the confine of the one-loop analysis.

The organization of the paper is as follows. In Sec. II, we analyze the minimal two-loop RG flow equation and in particular find that, as d varies, the fixed point goes through a Hopf bifurcation, resulting in a limit cycle with discrete scale invariance. There, a controversy in $d > d_{\rm u}$ [71] is also addressed. We then employ a coordinate-transformed RG scheme in Sec. III, within which the basin of attraction of the critical fixed point (or limit cycle) stays finite for all d, in contrast to previously reported scenarios [39,71]. We then briefly conclude in Sec. IV.

II. MINIMAL TWO-LOOP RG

The critical RSB transitions in spin and structural glasses are universally signaled by the instability of the replicon fluctuations, $\phi_{ab}(\mathbf{x})$ [13,18] (see Appendix A). The critical field theory for this de Almeida–Thouless–Gardner universality class is governed by two cubic couplings, $g^{\mathcal{X}=\mathrm{I,II}}$, with the bare Lagrangian

$$\mathcal{L} = \frac{1}{2}\sum_{a,b=1}^{n}(\nabla\phi_{ab})^2 - \frac{1}{3!}\left[g^{\rm I}\sum_{a,b=1}^{n}\phi_{ab}^3 + g^{\rm II}\sum_{a,b,c=1}^{n}\phi_{ab}\phi_{bc}\phi_{ca}\right]. \tag{1}$$

The β functions, $\beta^{\mathcal{X}} \equiv \mu\frac{\partial g^{\mathcal{X}}}{\partial\mu}$, then dictate the RG flow for these couplings. At two-loop order with the minimal subtraction scheme [39], we have

$$\begin{aligned}\beta^{\rm I} = {}& \frac{(d-6)}{2}g^{\rm I} - \frac{57}{16}(g^{\rm I})^3 + \frac{13}{2}(g^{\rm I})^2 g^{\rm II} - \frac{11}{4}g^{\rm I}(g^{\rm II})^2 \\ & - \frac{42293}{2304}(g^{\rm I})^5 + \frac{35639}{576}(g^{\rm I})^4 g^{\rm II} - \frac{22265}{288}(g^{\rm I})^3(g^{\rm II})^2 \\ & + \frac{11987}{288}(g^{\rm I})^2(g^{\rm II})^3 - \frac{1139}{144}g^{\rm I}(g^{\rm II})^4, \end{aligned} \tag{2}$$

$$\begin{aligned}\beta^{\rm II} = {}& \frac{(d-6)}{2}g^{\rm II} - \frac{1}{8}(g^{\rm I})^3 - \frac{25}{16}(g^{\rm I})^2 g^{\rm II} + \frac{7}{2}g^{\rm I}(g^{\rm II})^2 - \frac{3}{2}(g^{\rm II})^3 \\ & - \frac{571}{768}(g^{\rm I})^5 - \frac{11153}{2304}(g^{\rm I})^4 g^{\rm II} + \frac{25615}{1152}(g^{\rm I})^3(g^{\rm II})^2 \\ & - \frac{35879}{1152}(g^{\rm I})^2(g^{\rm II})^3 + \frac{5099}{288}g^{\rm I}(g^{\rm II})^4 - \frac{1931}{576}(g^{\rm II})^5. \end{aligned} \tag{3}$$

The RG flow stops at points with $\beta^{\mathcal{X}} = 0$, i.e., at fixed points. Such points live at the intersections of curves on which $\beta^{\rm I} = 0$ and those on which $\beta^{\rm II} = 0$. At one-loop order for $d < d_{\rm u}$, these curves only intersect at the unstable Gaussian fixed point $g^{\mathcal{X}} = 0$ [Fig. 1(a)], but at two-loop order they intersect further [Fig. 1(b)]. This intersection results in a strong-coupling fixed point, visible only beyond one-loop order, just like the Caswell–Banks–Zaks fixed point in non-Abelian gauge theories [40,41].

The flow geometry around the strong-coupling fixed point evolves with d. To study this dimensional dependence more carefully, we analyze the minimal two-loop RG flow Eqs. (2) and (3) numerically [72]. For $d \leqslant d_0 \approx 4.84$, the strong-coupling fixed point is stable. For $d_0 < d < d_{\rm H} \approx 5.41$, the fixed point is still stable but the stability exponents acquire imaginary parts, causing the flow to spiral into the fixed point.

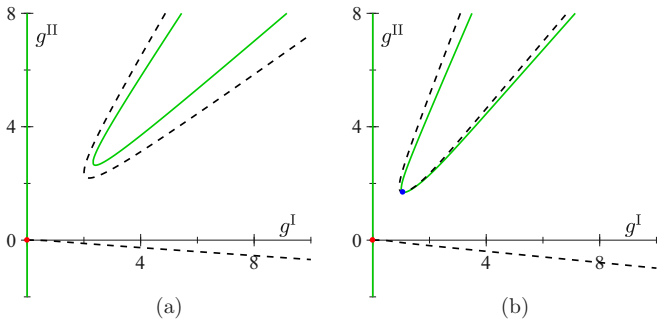

FIG. 1. Zeros of $\beta^{\rm I} = 0$ (green solid) and $\beta^{\rm II} = 0$ (black dashed) for $d = 3$. (a) At one-loop order, curves do not intersect except at the unstable Gaussian fixed point (red dot) at the origin. (b) At two-loop order, curves further intersect at the stable strong-coupling fixed point (blue dot).

At $d = d_{\rm H}$, the real part of the stability exponents changes sign, making the fixed point unstable and resulting in the emergence of a stable limit cycle through a Hopf bifurcation [Fig. 2(a)]. The limit cycle gives rise to a log-periodic, discrete scale invariance in physical observables such as two-point correlation functions right at the critical point. Scale invariance of this sort is familiar from the period-doubling route to chaos, and is speculated to be important in stock market crashes [73], earthquakes, and many other systems [74]. Our results indicate that spin and structural glasses might therefore share a connection with these phenomena.

The size of this stable limit cycle cascades toward infinity as dimension nears $d_{\rm cas} \approx 5.47$, and then an infinite remnant of the cycle persists [Fig. 2(b)]. For $d \in [d_{\rm cas}, d_{\rm u}]$, there is neither a stable fixed point nor a finite stable limit cycle in sight of the minimal two-loop analysis. Analytically continuing the flow equations above $d_{\rm u}$, the Gaussian fixed point becomes stable with a finite basin of attraction of size $\propto \sqrt{d - d_{\rm u}}$ [Fig. 2(c)], and at $d = d_{\rm col} \approx 6.01$ this basin collides with the infinite remnant of the limit cycle discussed above, resulting in a semi-infinite basin of attraction for the Gaussian fixed point [Fig. 2(d)].

In Ref. [71], through the analysis of the one-loop RG flow, Moore and Read predicted the existence of a multicritical point—and of a nonperturbative phase transition of an indeterminate kind—on the de Almeida-Thouless line. Their argument, which is based on the shrinkage of the basin of attraction as $d \to d_{\rm u}^+$ and the absence of the critical fixed point for $d < d_{\rm u}$ in the weak-coupling regime, still applies to the minimal two-loop RG flow in the window $d \in [d_{\rm cas}, d_{\rm col}) \approx [5.41, 6.01)$. In the next section, we suggest an alternative scenario that emerges upon transforming the coordinates of two-loop RG equations.

III. DEPENDENCE ON COORDINATE TRANSFORMATIONS

In Ref. [39], a three-loop calculation with Borel resummation was performed to further corroborate the existence of the critical fixed point identified at two-loop order. However, the resummation scheme employed was somewhat ad hoc, in part because of the scarcity of systematic studies on resummation

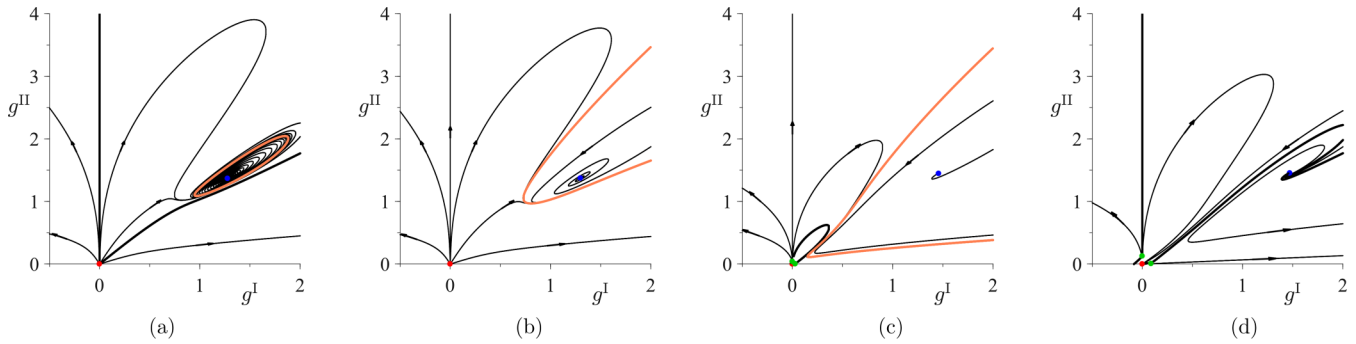

FIG. 2. Flows in the space of couplings for minimal two-loop RG equations. (a) At $d = 5.43 \in (d_{\mathrm{H}}, d_{\mathrm{cas}})$, a limit cycle (thick orange line) is observed around the strong coupling fixed point (blue dot). Its basin of attraction is delineated by thick black lines. (b) At $d = 5.50 \in [d_{\mathrm{cas}}, d_{\mathrm{u}}]$, an infinite-size remnant of the limit cycle is observed, but no stable fixed point. Within the remnant, the flow emanates from the strong-coupling fixed point and then circles around and approaches this infinite remnant. (c) At $d = 6.005 \in (d_{\mathrm{u}}, d_{\mathrm{col}})$, the Gaussian fixed point (red dot) is stable with a finite basin of attraction. On the boundary of the basin, two unstable fixed points (green dots) are observed along with their mirror images. (d) At $d = 6.05 \geqslant d_{\mathrm{col}}$, the finite Gaussian basin and the infinite-size remnant of the limit cycle have merged. The Gaussian basin is now semi-infinite.

schemes for field theories with two couplings (see, however, Ref. [75]). Nonperturbative RG equations also exist for this problem (see Appendix B). Although a partial analysis suggests that their predictions are consistent with those of the two-loop analysis, the results also suffer from the uncontrolled scheme dependence. Just as for the Ising universality class, the existence and nature of the fixed point thus depend on the details of the scheme used. The coordinate-transformation scheme we present below is no exception to this lack of systematics. It nonetheless yields a simple scenario, in which the critical RSB transition survives for all spatial dimensions d. The proposal should thus be of interest for the community to keep in mind.

Generically, external parameters controlled in experiments and simulations map nontrivially to coupling coordinates of effective field theories in the RG analysis. It is therefore natural to analyze the dependence of the fixed point structure against changes in coupling coordinates. In particular, universal properties near a fixed point should be invariant under coordinate changes, and this invariance can be used to cast the RG equations into a normal form around that fixed point [76]. Below, we perform a coordinate change around the Gaussian fixed point and explore its effect on the strong-coupling fixed point.

Scrutinizing the structure of Feynman diagrams lets us organize the perturbative two-loop RG flow equation into the form [39]

$$\mu\frac{\partial g^{\mathcal{X}}}{\partial\mu} = \left[-\frac{\epsilon}{2} + \frac{1}{4}I_2(g) - \frac{11}{144}I_2^2(g) + \frac{1}{6}I_4(g)\right]g^{\mathcal{X}} - I_3^{\mathcal{X}}(g) + \frac{7}{24}I_2(g)I_3^{\mathcal{X}}(g) - \frac{1}{2}I_{5,A}^{\mathcal{X}}(g) - \frac{3}{4}I_{5,B}^{\mathcal{X}}(g), \tag{4}$$

where $\epsilon \equiv d_{\mathrm{u}} - d$ and $I_k(g)$'s are kth degree homogeneous polynomials of two variables $g^{\mathcal{X}=\mathrm{I,II}}$ (see Appendix A). We keep this algebraic structure suggested by the Feynman diagrams intact and thus restrict ourselves to the class of coordinate transformations involving only these polynomials. Specifically, we recast the RG-flow equations in a new normal-form coordinate $\tilde{g}^{\mathcal{X}}$ defined through

$$g^{\mathcal{X}} = \tilde{g}^{\mathcal{X}} + \lambda_1\tilde{g}^{\mathcal{X}}I_2(\tilde{g}) + \lambda_2 I_3^{\mathcal{X}}(\tilde{g}) + \Lambda_1\tilde{g}^{\mathcal{X}}I_2^2(\tilde{g}) + \Lambda_2\tilde{g}^{\mathcal{X}}I_4(\tilde{g}) + \Lambda_3 I_2(\tilde{g})I_3^{\mathcal{X}}(\tilde{g}) + \Lambda_4 I_{5,A}^{\mathcal{X}}(\tilde{g}) + \Lambda_5 I_{5,B}^{\mathcal{X}}(\tilde{g}) + O(\tilde{g}^7) \tag{5}$$

and truncate higher-order terms. Here, coefficients $\lambda_{1,2}$ and $\Lambda_{1,2,\ldots,5}$ are real parameters of the coordinate transformation. After some algebra we obtain

$$\mu\frac{\partial\tilde{g}^{\mathcal{X}}}{\partial\mu} = \left\{-\frac{\epsilon}{2} + \left(\frac{1}{4}+\epsilon\lambda_1\right)I_2(\tilde{g}) + \left[-\frac{11}{144} + \epsilon\left(-3\lambda_1^2 + 2\Lambda_1\right)\right]I_2^2(\tilde{g}) + \left[\frac{1}{6} + 2\lambda_1 + \frac{1}{2}\lambda_2 + \epsilon(-2\lambda_1\lambda_2 + 2\Lambda_2)\right]I_4(\tilde{g})\right\}\tilde{g}^{\mathcal{X}} + (-1+\epsilon\lambda_2)I_3^{\mathcal{X}}(\tilde{g}) + \left[\frac{7}{24} - 2\lambda_1 - \frac{1}{2}\lambda_2 + \epsilon(-4\lambda_1\lambda_2 + 2\Lambda_3)\right]I_2(\tilde{g})I_3^{\mathcal{X}}(\tilde{g}) + \left(-\frac{1}{2} + 2\epsilon\Lambda_4\right)I_{5,A}^{\mathcal{X}}(\tilde{g}) + \left[-\frac{3}{4} + \epsilon\left(-3\lambda_2^2 + 2\Lambda_5\right)\right]I_{5,B}^{\mathcal{X}}(\tilde{g}) + O(\tilde{g}^7). \tag{6}$$

Here, we choose $\Lambda_{1,2,3,4,5}$ appropriately to cancel the ϵ-dependent quintic terms, which yields

$$\mu\frac{\partial\tilde{g}^{\mathcal{X}}}{\partial\mu} = \left[-\frac{\epsilon}{2} + \left(\frac{1}{4}+\epsilon\lambda_1\right)I_2(\tilde{g}) - \frac{11}{144}I_2^2(\tilde{g}) + \left(\frac{1}{6} + 2\lambda_1 + \frac{1}{2}\lambda_2\right)I_4(\tilde{g})\right]\tilde{g}^{\mathcal{X}} + (-1+\epsilon\lambda_2)I_3^{\mathcal{X}}(\tilde{g}) + \left(\frac{7}{24} - 2\lambda_1 - \frac{1}{2}\lambda_2\right)I_2(\tilde{g})I_3^{\mathcal{X}}(\tilde{g}) - \frac{1}{2}I_{5,A}^{\mathcal{X}}(\tilde{g}) - \frac{3}{4}I_{5,B}^{\mathcal{X}}(\tilde{g}) + O(\tilde{g}^7). \tag{7}$$

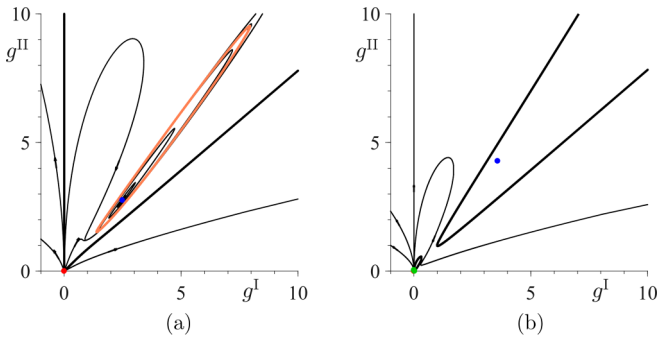

FIG. 3. Flows in the space of couplings for the coordinate-transformed two-loop RG scheme, with $\lambda_1 = -0.55$ and $\lambda_2 = 0$. (a) At $d = 3$, a limit cycle (thick orange line) is observed around the strong coupling fixed point. Its basin of attraction is delineated by thick black lines. (b) At $d = 6.005$, two basins of attraction are observed: one for the Gaussian fixed point and the other for the strong-coupling fixed point.

For $d = d_{\mathrm{u}}$ the flow equation depends only on one parameter, the linear combination $\lambda \equiv -2\lambda_1 - \frac{1}{2}\lambda_2$:

$$\mu\frac{\partial\tilde{g}^{\mathcal{X}}}{\partial\mu} = \left[\frac{1}{4}I_2(\tilde{g}) - \frac{11}{144}I_2^2(\tilde{g}) + \left(\frac{1}{6} - \lambda\right)I_4(\tilde{g})\right]\tilde{g}^{\mathcal{X}} - I_3^{\mathcal{X}}(\tilde{g}) + \left(\frac{7}{24} + \lambda\right)I_2(\tilde{g})I_3^{\mathcal{X}}(\tilde{g}) - \frac{1}{2}I_{5,A}^{\mathcal{X}}(\tilde{g}) - \frac{3}{4}I_{5,B}^{\mathcal{X}}(\tilde{g}) + O(\tilde{g}^7). \tag{8}$$

The existence of the strong-coupling fixed point is robust against λ-deformation within the window $\lambda \in [-0.91, 1.19]$. In addition, the fixed point becomes stable for $\lambda > \lambda_{\mathrm{aH}} \approx 1.00$ through an anti-Hopf bifurcation. In other words, for $\lambda < \lambda_{\mathrm{aH}}$ the fixed point is unstable without a limit cycle around it, while for $\lambda > \lambda_{\mathrm{aH}}$ it is stable with an unstable limit cycle around it.

For $d \neq d_{\mathrm{u}}$, the space of coordinate changes is two dimensional. While this restricted space is much simpler than the full space of coordinate changes (recall that we chose to respect the algebraic structure mentioned above and chose to cancel ϵ-dependences of the highest-order terms in the RG equations), there are still a myriad of possibilities depending on the values of $\lambda_{1,2}$ (and $\lambda_{1,2}$ can even depend on d). We will not thoroughly investigate these possibilities because, without a guiding principle to dictate the desired properties of the coordinate transformation, such effort would be mostly moot. Instead, below we illustrate one particular physical scenario given by the specific choice $\lambda_1 = -0.55$ and $\lambda_2 = 0$. For this choice and for d just above d_{u}, two basins of attractions can be found: one for the Gaussian fixed point and the other for the strong-coupling fixed point, which is stable here due to our choice $\lambda = 1.1 \in (\lambda_{\mathrm{aH}}, 1.19]$ [Fig. 3(b)]. There, depending on the microscopic details of the model, the de Almeida–Thouless–Gardner critical line may then do one of the following: (i) lie completely within the Gaussian basin, in which case one observes the mean-field criticality; (ii) lie completely within the strong-coupling basin, in which case one observes non-mean-field criticality; (iii) cross borders of basins, in which case the line fragments into several parts; or (iv) not lie within any basin, in which case one might not observe any criticality.

As $d \to d_{\mathrm{u}}^+$, the Gaussian basin shrinks to zero while the strong-coupling basin remains nonzero. Upon further decreasing d, with $(\lambda_1, \lambda_2) = (-0.55, 0)$ the strong-coupling fixed point goes through a Hopf bifurcation at $d \approx 4.87$, below which it has a stable limit cycle around it [Fig. 3(a)]. Note that this process is the opposite of what happens within the minimal two-loop RG scheme, in which the Hopf bifurcation results in the limit cycle upon increasing d. In contrast, at least for the specific coordinate-transformation scheme under discussion, discrete scale invariance is here observed in low dimensions. Interestingly, a nontrivial critical fixed point in high dimension was also found in Ref. [34], within a Migdal-Kadanoff RG scheme, but no critical limit cycle was then found upon lowering dimensions.

In summary, with this choice of transformation, the basin of attraction for the strong-coupling criticality stays nonzero around and below the upper critical dimension and, if a given model lies within it for all d, a dimensionally robust nontrivial criticality is expected.

IV. CONCLUSION

We have analyzed the higher-loop RG flow equations for the critical RSB transitions to explore scenarios that are invisible at one-loop order. The analysis of the minimal two-loop RG flow equations reveals a strong-coupling critical fixed point, as first reported in Ref. [39], and a more careful analysis of their dimensional dependence discloses a critical limit cycle in a certain range of dimensions. In addition we have partly explored the range of possible extrapolation of the perturbative RG calculations far from the Gaussian fixed point, especially through their dependence on the choice of perturbative coordinate changes in coupling space. For the critical RSB field theory analyzed herein, such coordinate transformations of the two-loop equation depict several plausible physical predictions, one of which suggests that the basin of attraction of the critical RSB transition stays nonzero in all spatial dimensions d, with a limit cycle in lower dimensions. These scheme dependencies highlight the need for further development in resummed, coordinate-transformed, and nonperturbative RG schemes. The critical RSB field theory should serve as a key testing ground for these advances.

In addition to persistent theoretical investigations, experiments and simulations on a diverse set of systems will be indispensable to determine the role of RSB transitions in finite dimensions. To emphasize this point, let us imagine a given model that lies close to the Gaussian fixed point. In that case, even if a strong-coupling fixed point exists, the one-loop scenario would still apply, with the de Almeida-Thouless line fragmenting upon $d \to d_{\mathrm{u}}^+$, as proposed in Ref. [71] and criticality being absent below d_{u}. It is also possible that a given model might stay outside the basins of the critical fixed points, in which case it would not exhibit any sign of criticality, just as in the droplet scenario. These considerations show that an absence of RSB criticality in a few model systems may be due to their unfortunate locations in coupling space and thus cannot be invoked to exclude the presence of criticality in other systems. By contrast, a single observation

of RSB criticality for $d < d_{\rm u}$ would indicate the existence of a nontrivial critical fixed point. In particular, if discrete scale invariance were observed in any dimension, it would substantially support the strong-coupling criticality scenario proposed in Ref. [39] and further explored herein.

Data associated with this work are available from the Duke Digital Repository [77].

ACKNOWLEDGMENTS

We thank Giulio Biroli and Michael A. Moore for discussions. P.C., Y.H., and S.Y. acknowledge support from the Simons Foundation Grant No. 454937 (P.C.), and J.P.S. and A.R. acknowledge support from the National Science Foundation Grant No. NSF DMR-1719490.

APPENDIX A: COMBINATORIAL FACTORS

As discussed in Ref. [39], the critical replicon field, $\phi_{ab}(\mathbf{x})$, is symmetric, i.e., $\phi_{ab} = \phi_{ba}$ for replica indices a, b running from 1 to n, has no diagonal degree of freedom, i.e., $\phi_{aa} = 0$, and further satisfies the replicon conditions $\sum_{b=1}^{n} \phi_{ab} = 0$. By defining an orthonormal basis $\{e^i_{ab}\}_{i=1,\ldots,n(n-3)/2}$ through

$$\sum_{a,b=1}^{n} e^i_{ab} e^j_{ab} = \delta^{ij}, \tag{A1}$$

$$e^i_{aa} = 0, \tag{A2}$$

and

$$\sum_{b=1}^{n} e^i_{ab} = 0 \tag{A3}$$

for all $a = 1, \ldots, n$, we can expand the replicon field as

$$\phi_{ab}(\mathbf{x}) = \sum_{i=1}^{\frac{n(n-3)}{2}} \phi_i(\mathbf{x}) e^i_{ab}. \tag{A4}$$

The critical Lagrangian can then be expressed as

$$\begin{aligned}\mathcal{L} &= \frac{1}{2}\sum_{a,b=1}^{n} (\nabla\phi_{ab})^2 - \frac{1}{3!}\left(g^{\rm I} \sum_{a,b=1}^{n} \phi^3_{ab} + g^{\rm II} \sum_{a,b,c=1}^{n} \phi_{ab}\phi_{bc}\phi_{ca} \right) \\ &= \frac{1}{2}\sum_{i=1}^{\frac{n(n-3)}{2}} (\nabla\phi_i)^2 - \frac{1}{3!}\sum_{i,j,k=1}^{\frac{n(n-3)}{2}} \left(g^{\rm I} T^{ijk}_{\rm I} + g^{\rm II} T^{ijk}_{\rm II} \right) \phi_i\phi_j\phi_k,\end{aligned} \tag{A5}$$

with

$$T^{ijk}_{\rm I} \equiv \sum_{a,b=1}^{n} e^i_{ab} e^j_{ab} e^k_{ab} \tag{A6}$$

and

$$T^{ijk}_{\rm II} \equiv \sum_{a,b,c=1}^{n} e^i_{ab} e^j_{bc} e^k_{ca}. \tag{A7}$$

The homogeneous polynomials that appear in Eq. (4) are defined as

$$I_2(g) \equiv \sum_{\mathcal{X}_1,\mathcal{X}_2\in\{\rm I,II\}} S_{\mathcal{X}_1,\mathcal{X}_2} g^{\mathcal{X}_1} g^{\mathcal{X}_2}, \tag{A8}$$

$$I^{\mathcal{X}}_3(g) \equiv \sum_{\mathcal{X}_1,\mathcal{X}_2,\mathcal{X}_3\in\{\rm I,II\}} a^{\mathcal{X}}_{\mathcal{X}_1,\mathcal{X}_2,\mathcal{X}_3} g^{\mathcal{X}_1} g^{\mathcal{X}_2} g^{\mathcal{X}_3}, \tag{A9}$$

$$I_4(g) \equiv \sum_{\mathcal{X}_1,\mathcal{X}_2,\mathcal{X}_3,\mathcal{X}_4,\mathcal{X}_5\in\{\rm I,II\}} S_{\mathcal{X}_1,\mathcal{X}_5} a^{\mathcal{X}_5}_{\mathcal{X}_2,\mathcal{X}_3,\mathcal{X}_4} g^{\mathcal{X}_1} g^{\mathcal{X}_2} g^{\mathcal{X}_3} g^{\mathcal{X}_4}, \tag{A10}$$

$$I^{\mathcal{X}}_{5,A}(g) \equiv \sum_{\mathcal{X}_1,\mathcal{X}_2,\mathcal{X}_3,\mathcal{X}_4,\mathcal{X}_5\in\{\rm I,II\}} a^{\mathcal{X}}_{\mathcal{X}_1,\mathcal{X}_2,\mathcal{X}_3;\mathcal{X}_4,\mathcal{X}_5} g^{\mathcal{X}_1} g^{\mathcal{X}_2} g^{\mathcal{X}_3} g^{\mathcal{X}_4} g^{\mathcal{X}_5}, \tag{A11}$$

$$\begin{aligned}I^{\mathcal{X}}_{5,B}(g) \equiv &\sum_{\mathcal{X}_1,\mathcal{X}_2,\mathcal{X}_3,\mathcal{X}_4,\mathcal{X}_5,\mathcal{X}_6\in\{\rm I,II\}} a^{\mathcal{X}}_{\mathcal{X}_1,\mathcal{X}_2,\mathcal{X}_6} a^{\mathcal{X}_6}_{\mathcal{X}_3,\mathcal{X}_4,\mathcal{X}_5} g^{\mathcal{X}_1} g^{\mathcal{X}_2} \\ &\times g^{\mathcal{X}_3} g^{\mathcal{X}_4} g^{\mathcal{X}_5}.\end{aligned} \tag{A12}$$

The one-loop self-energy combinatorial factors, defined through

$$\sum_{i_3,i_4=1}^{\frac{n(n-3)}{2}} T^{i_1 i_3 i_4}_{\mathcal{X}_1} T^{i_2 i_4 i_3}_{\mathcal{X}_2} = S_{\mathcal{X}_1,\mathcal{X}_2} \delta^{i_1 i_2}, \tag{A13}$$

satisfies $S_{\mathcal{X}_1,\mathcal{X}_2} = S_{\mathcal{X}_2,\mathcal{X}_1}$, the one-loop cubic factors $a^{\mathcal{X}}_{\mathcal{X}_1,\mathcal{X}_2,\mathcal{X}_3}$, defined through

$$\sum_{i_4,i_5,i_6=1}^{\frac{n(n-3)}{2}} T^{i_1 i_5 i_6}_{\mathcal{X}_1} T^{i_2 i_6 i_4}_{\mathcal{X}_2} T^{i_3 i_4 i_5}_{\mathcal{X}_3} = \sum_{\mathcal{X}\in\{\rm I,II\}} a^{\mathcal{X}}_{\mathcal{X}_1,\mathcal{X}_2,\mathcal{X}_3} T^{i_1 i_2 i_3}_{\mathcal{X}}, \tag{A14}$$

are symmetric under permutations of indices $(\mathcal{X}_1, \mathcal{X}_2, \mathcal{X}_3)$, and the two-loop cubic factors $a^{\mathcal{X}}_{\mathcal{X}_1,\mathcal{X}_2,\mathcal{X}_3;\mathcal{X}_4,\mathcal{X}_5}$, defined through

$$\begin{aligned}&\sum_{i_4,i_5,i_6,i_7,i_8,i_9=1}^{\frac{n(n-3)}{2}} T^{i_1 i_5 i_6}_{\mathcal{X}_1} T^{i_2 i_4 i_8}_{\mathcal{X}_2} T^{i_3 i_7 i_9}_{\mathcal{X}_3} T^{i_4 i_6 i_9}_{\mathcal{X}_4} T^{i_5 i_7 i_8}_{\mathcal{X}_5} \\ &\quad\equiv \sum_{\mathcal{X}\in\{\rm I,II\}} a^{\mathcal{X}}_{\mathcal{X}_1,\mathcal{X}_2,\mathcal{X}_3;\mathcal{X}_4,\mathcal{X}_5} T^{i_1 i_2 i_3}_{\mathcal{X}},\end{aligned} \tag{A15}$$

are symmetric under permutations of the first three indices $(\mathcal{X}_1, \mathcal{X}_2, \mathcal{X}_3)$ and of the last two indices $(\mathcal{X}_4, \mathcal{X}_5)$. Explicitly, these combinatorial factors are given by (as taken from Ref. [39])

$$\begin{bmatrix} S_{\rm I,I} \\ S_{\rm I,II} \\ S_{\rm II,II} \end{bmatrix} = \begin{bmatrix} \frac{n^3-9n^2+26n-22}{2(n-1)(n-2)^2} \\ \frac{3n^2-15n+16}{2(n-1)(n-2)^2} \\ \frac{n^4-8n^3+19n^2-4n-16}{4(n-1)(n-2)^2} \end{bmatrix}, \tag{A16}$$

$$\begin{bmatrix} a^{\mathrm{I}}_{\mathrm{I,I,I}} & a^{\mathrm{II}}_{\mathrm{I,I,I}} \\ a^{\mathrm{I}}_{\mathrm{I,I,II}} & a^{\mathrm{II}}_{\mathrm{I,I,II}} \\ a^{\mathrm{I}}_{\mathrm{I,II,II}} & a^{\mathrm{II}}_{\mathrm{I,II,II}} \\ a^{\mathrm{I}}_{\mathrm{II,II,II}} & a^{\mathrm{II}}_{\mathrm{II,II,II}} \end{bmatrix} = \begin{bmatrix} \frac{n^3-11n^2+38n-34}{2(n-1)(n-2)^2} & \frac{-1}{(n-2)^3} \\ \frac{3n^2-19n+20}{2(n-1)(n-2)^2} & \frac{-n^3+8n^2-17n+12}{2(n-1)(n-2)^3} \\ \frac{-n^3+5n^2+8n-16}{4(n-1)(n-2)^2} & \frac{3n^3-27n^2+64n-48}{4(n-1)(n-2)^3} \\ \frac{-3n}{2(n-2)^2} & \frac{n^5-10n^4+33n^3-8n^2-104n+112}{8(n-1)(n-2)^3} \end{bmatrix}, \tag{A17}$$

$$\begin{bmatrix} a^{\mathrm{I}}_{\mathrm{I,I,I;I,I}} \\ a^{\mathrm{I}}_{\mathrm{II,I,I;I,I}} \\ a^{\mathrm{I}}_{\mathrm{I,I,I;II,I}} \\ a^{\mathrm{I}}_{\mathrm{I,I,I;II,II}} \\ a^{\mathrm{I}}_{\mathrm{II,II,I;I,I}} \\ a^{\mathrm{I}}_{\mathrm{II,I,I;II,I}} \\ a^{\mathrm{I}}_{\mathrm{II,II,II;I,I}} \\ a^{\mathrm{I}}_{\mathrm{I,I,II;II,II}} \\ a^{\mathrm{I}}_{\mathrm{I,II,II;I,II}} \\ a^{\mathrm{I}}_{\mathrm{I,II,II;II,II}} \\ a^{\mathrm{I}}_{\mathrm{II,II,II;I,II}} \\ a^{\mathrm{I}}_{\mathrm{II,II,II;II,II}} \end{bmatrix} \equiv \begin{bmatrix} \frac{n^8-26n^7+291n^6-1816n^5+6840n^4-15756n^3+21586n^2-16088n+5008}{4(n-1)^2(n-2)^6} \\ \frac{3n^7-66n^6+607n^5-2960n^4+8132n^3-12592n^2+10236n-3392}{4(n-1)^2(n-2)^6} \\ \frac{3n^7-66n^6+604n^5-2930n^4+8017n^3-12380n^2+10048n-3328}{4(n-1)^2(n-2)^6} \\ \frac{21n^6-366n^5+2493n^4-8316n^3+14536n^2-12800n+4480}{8(n-1)^2(n-2)^6} \\ \frac{3n^7-27n^6-59n^5+1471n^4-6396n^3+12496n^2-11664n+4224}{8(n-1)^2(n-2)^6} \\ \frac{n^7-7n^6-63n^5+819n^4-3292n^3+6262n^2-5776n+2080}{4(n-1)^2(n-2)^6} \\ \frac{n^9-19n^8+145n^7-541n^6+1018n^5-1488n^4+4292n^3-10192n^2+11328n-4608}{16(n-1)^2(n-2)^6} \\ \frac{-n^7+20n^6-110n^5+84n^4+871n^3-2704n^2+3040n-1216}{4(n-1)^2(n-2)^6} \\ \frac{-7n^7+134n^6-819n^5+1708n^4+680n^3-7552n^2+10144n-4352}{16(n-1)^2(n-2)^6} \\ \frac{n^9-15n^8+95n^7-469n^6+2196n^5-6368n^4+8592n^3-2176n^2-5376n+3584}{32(n-1)^2(n-2)^6} \\ \frac{3n^8-42n^7+169n^6+68n^5-1750n^4+3488n^3-1456n^2-1984n+1536}{16(n-1)^2(n-2)^6} \\ \frac{n(-3n^6+54n^5-315n^4+560n^3+376n^2-1968n+1440)}{16(n-1)(n-2)^6} \end{bmatrix}, \tag{A18}$$

and

$$\begin{bmatrix} a^{\mathrm{II}}_{\mathrm{I,I,I;I,I}} \\ a^{\mathrm{II}}_{\mathrm{II,I,I;I,I}} \\ a^{\mathrm{II}}_{\mathrm{I,I,I;II,I}} \\ a^{\mathrm{II}}_{\mathrm{I,I,I;II,II}} \\ a^{\mathrm{II}}_{\mathrm{II,II,I;I,I}} \\ a^{\mathrm{II}}_{\mathrm{II,I,I;II,I}} \\ a^{\mathrm{II}}_{\mathrm{II,II,II;I,I}} \\ a^{\mathrm{II}}_{\mathrm{I,I,II;II,II}} \\ a^{\mathrm{II}}_{\mathrm{I,II,II;I,II}} \\ a^{\mathrm{II}}_{\mathrm{I,II,II;II,II}} \\ a^{\mathrm{II}}_{\mathrm{II,II,II;I,II}} \\ a^{\mathrm{II}}_{\mathrm{II,II,II;II,II}} \end{bmatrix} \equiv \begin{bmatrix} \frac{3(n^2-7n+8)}{(n-1)^1(n-2)^5} \\ \frac{n^5-15n^4+78n^3-165n^2+159n-62}{2(n-1)^2(n-2)^5} \\ \frac{3n^5-42n^4+211n^3-448n^2+436n-168}{4(n-1)^2(n-2)^5} \\ \frac{n^7-18n^6+127n^5-420n^4+574n^3-40n^2-608n+416}{8(n-1)^2(n-2)^5} \\ \frac{-n^5+19n^4-118n^3+296n^2-336n+148}{2(n-1)^2(n-2)^5} \\ \frac{-2n^5+41n^4-260n^3+659n^2-750n+328}{4(n-1)^2(n-2)^5} \\ \frac{3n^5-72n^4+531n^3-1494n^2+1848n-864}{8(n-1)^2(n-2)^5} \\ \frac{3n^6-39n^5+151n^4-45n^3-726n^2+1344n-736}{8(n-1)^2(n-2)^5} \\ \frac{n^7-14n^6+81n^5-352n^4+1412n^3-3384n^2+3984n-1824}{16(n-1)^2(n-2)^5} \\ \frac{3n^5-17n^4-25n^3+243n^2-420n+232}{2(n-1)^2(n-2)^5} \\ \frac{3n^6-24n^5+147n^4-1006n^3+3136n^2-4240n+2112}{16(n-1)^2(n-2)^5} \\ \frac{3n^8-47n^7+315n^6-1229n^5+3110n^4-4088n^3+336n^2+4928n-3648}{32(n-1)^2(n-2)^5} \end{bmatrix}. \tag{A19}$$

APPENDIX B: NONPERTURBATIVE RG

We consider here the replicon field theory from the nonperturbative RG approach proposed by Wetterich [62]. This scheme uses the Legendre transform of the Polchinski equation [61], casting the exact RG equations in a way that naturally leads to various approximation schemes. As such, it has had success with the Lifshitz critical point [78], random-field spin models [65,79,80], fully developed turbulent flows [81], and others [64,66].

More specifically, within the nonperturbative RG scheme [64,66], the microscopic action $S_\Lambda[\phi]$ is supplemented by a cutoff term

$$\Delta S[\phi] = \frac{1}{2}\int \frac{d\mathbf{q}}{(2\pi)^d} R_\mu(\mathbf{q}^2) \sum_{i=1}^{\frac{n(n-3)}{2}} \phi_i(\mathbf{q})\phi_i(-\mathbf{q}), \tag{B1}$$

where the scale-dependent cutoff function, $R_\mu(\mathbf{q}^2)$, suppresses *low*-momentum fluctuations, i.e., with $|\mathbf{q}| \lesssim \mu$ [*cf.* Eq. (B30)].

The resulting one-particle-irreducible effective action, $\Gamma_\mu[\phi]$, then obeys the Wetterich equation [62]

$$\mu\frac{\partial}{\partial\mu}\Gamma_\mu[\phi] = \frac{1}{2}\int\frac{d\mathbf{q}}{(2\pi)^d}\left\{\mu\frac{\partial}{\partial\mu}R_\mu(\mathbf{q}^2)\right\} \times \sum_{i=1}^{\frac{n(n-3)}{2}}\left\{\left(\Gamma_\mu^{(2)}[\phi]+R_\mu\mathbb{1}\right)^{-1}\right\}_{i,i}(\mathbf{q},\mathbf{q}), \quad \text{(B2)}$$

where

$$\left(\Gamma_\mu^{(2)}[\phi]\right)_{i,j}(\mathbf{q},\mathbf{q}') \equiv \frac{\delta^2\Gamma_\mu[\phi]}{\delta\phi_i(-\mathbf{q})\delta\phi_j(\mathbf{q}')} \quad \text{(B3)}$$

and

$$(R_\mu\mathbb{1})_{i,j}(\mathbf{q},\mathbf{q}') \equiv R_\mu(\mathbf{q}^2)\delta_{ij}(2\pi)^d\delta^{(d)}(\mathbf{q}-\mathbf{q}'). \quad \text{(B4)}$$

Although the Wetterich equation is exact, it is intractable in practice. As mentioned above, it nonetheless provides a natural starting point for devising various approximation schemes. We here adopt the most commonly employed scheme, the pseudolocal potential approximation, which implements the derivative expansion on the one-particle-irreducible effective action. To make the analysis tractable in presence of complex index structures, we further truncate the potential-energy term. We find that the strict truncation to cubic order produces a behavior qualitatively similar to one-loop perturbative calculations without stable fixed points for $d < d_\mathrm{u}$, while the inclusion of quartic terms as independent couplings results in a plethora of spurious, unphysical fixed points, as was also observed in simpler models [82]. To correctly treat higher-order contributions, we thus follow the systematic approach of Ref. [83], which reproduces two-loop results for $d = d_\mathrm{u}$ when perturbatively expanded in couplings, while being similarly robust both at weak and strong couplings; see also Refs. [63,82] for different schemes.

Note that to fully imitate the approach of Ref. [83] and, in particular, to successfully reproduce the two-loop results in the weak-coupling limit we need to expand terms around the vacuum expectation value of a generic RSB phase and include more derivative terms. Because properly treating Nambu-Goldstone soft modes around a RSB phase remains an open problem, what follows is a simplified scheme. We have nonetheless checked that the results are qualitatively robust against various changes of the scheme: (i) excluding the quintic term, $\frac{1}{5!}\sum_{i_1,\ldots,i_5=1}^{\frac{n(n-3)}{2}}\tilde{V}^{i_1i_2i_3i_4i_5}_{(5)*}\phi_{i_1}\phi_{i_2}\phi_{i_3}\phi_{i_4}\phi_{i_5}$; (ii) including the cubic term with two derivatives, $\frac{1}{2}\sum_{i_1,j_1,j_2=1}^{\frac{n(n-3)}{2}}\tilde{D}^{i_1|j_1j_2}_{(3)*}\phi_{i_1}(\nabla\phi_{j_1})(\nabla\phi_{j_2})$; (iii) including both cubic and quartic terms with two derivatives, the latter having the form of $\frac{1}{4}\sum_{i_1,i_2,j_1,j_2=1}^{\frac{n(n-3)}{2}}\tilde{D}^{i_1i_2|j_1j_2}_{(4)*}\phi_{i_1}\phi_{i_2}(\nabla\phi_{j_1})(\nabla\phi_{j_2})$; (iv) including all cubic, quartic, and quintic terms with two derivatives, the last having the form of $\frac{1}{12}\sum_{i_1,i_2,i_3,j_1,j_2=1}^{\frac{n(n-3)}{2}}\tilde{D}^{i_1i_2,i_3|j_1j_2}_{(5)*}\phi_{i_1}\phi_{i_2}\phi_{i_3}(\nabla\phi_{j_1})(\nabla\phi_{j_2})$; and (v) changing the sharp cutoff function, Eq. (B30), to a smooth $R_\mu(\mathbf{q}^2) = \frac{Z_\mu\mathbf{q}^2}{\exp(\mathbf{q}^2/\mu^2)-1}$. Of these, only (iv) qualitatively changed the results, but this interference and the quantitative disagreement with other approaches mentioned in the main text would be likely cured if effects of the vacuum expectation value were properly included.

Within this approach, the effective action contains two parts, $\Gamma_\mu[\phi] = \Gamma_\mu^{\mathrm{primary}}[\phi] + \tilde{\Gamma}_*[\phi]$. The first is the primary action

$$\Gamma_\mu^{\mathrm{primary}}[\phi] = \int d\mathbf{x}\left\{\frac{Z_\mu}{2}\sum_{i=1}^{\frac{n(n-3)}{2}}(\nabla\phi_i)^2 + \frac{\tilde{r}_\mu}{2}\sum_{i=1}^{\frac{n(n-3)}{2}}\phi_i^2 - \frac{1}{3!}\sum_{i_1,i_2,i_3=1}^{\frac{n(n-3)}{2}}\left(\sum_{\mathcal{X}\in\{\mathrm{I},\mathrm{II}\}}\tilde{g}_\mu^{\mathcal{X}}T_{\mathcal{X}}^{i_1i_2i_3}\right)\phi_{i_1}\phi_{i_2}\phi_{i_3}\right\}, \quad \text{(B5)}$$

governed by independent couplings, $\{Z_\mu, \tilde{r}_\mu, \tilde{g}_\mu^{\mathcal{X}}\}$. The second is the one-loop improved action

$$\tilde{\Gamma}_*[\phi] = \frac{1}{2}\int\frac{d\mathbf{q}}{(2\pi)^d}\sum_{i=1}^{\frac{n(n-3)}{2}}\left\{\ln\left(\Gamma_\mu^{\mathrm{primary}(2)}[\phi]+R_\mu\mathbb{1}\right)\right\}_{i,i}(\mathbf{q},\mathbf{q}), \quad \text{(B6)}$$

from which we discard terms that are already contained in the primary action. The secondary action can then be written as

$$\tilde{\Gamma}_*[\phi] = \int d\mathbf{x}\left\{\frac{1}{4!}\sum_{i_1,i_2,i_3,i_4=1}^{\frac{n(n-3)}{2}}\tilde{V}^{i_1i_2i_3i_4}_{(4)*}\phi_{i_1}\phi_{i_2}\phi_{i_3}\phi_{i_4} - \frac{1}{5!}\sum_{i_1,\ldots,i_5=1}^{\frac{n(n-3)}{2}}\tilde{V}^{i_1i_2i_3i_4i_5}_{(5)*}\phi_{i_1}\phi_{i_2}\phi_{i_3}\phi_{i_4}\phi_{i_5}\right\}. \quad \text{(B7)}$$

Here, terms beyond the quintic order do not affect the renormalization-group equations for independent couplings and are thus suppressed.

To express secondary couplings as functions of independent couplings, we first expand the logarithm in the prescription of Eq. (B6). At ℓth order in ϕ, the one-loop improved action is given by

$$\frac{(-1)}{2\ell}\sum_{\mathcal{X}_1,\ldots,\mathcal{X}_\ell\in\{\mathrm{I},\mathrm{II}\}}\sum_{i_1,\ldots,i_\ell=1}^{\frac{n(n-3)}{2}}\tilde{g}_\mu^{\mathcal{X}_1}\tilde{g}_\mu^{\mathcal{X}_2}\cdots\tilde{g}_\mu^{\mathcal{X}_\ell}\omega^{i_1i_2\ldots i_\ell}_{\mathcal{X}_1,\mathcal{X}_2,\ldots,\mathcal{X}_\ell} \times\int\frac{d\mathbf{q}_1}{(2\pi)^d}\frac{d\mathbf{q}_2}{(2\pi)^d}\cdots\frac{d\mathbf{q}_\ell}{(2\pi)^d}A_0(\mathbf{q}_1^2)A_0(\mathbf{q}_2^2)\cdots A_0(\mathbf{q}_\ell^2) \times\phi_{i_1}(\mathbf{q}_\ell-\mathbf{q}_1)\phi_{i_2}(\mathbf{q}_1-\mathbf{q}_2)\cdots\phi_{i_\ell}(\mathbf{q}_{\ell-1}-\mathbf{q}_\ell), \quad \text{(B8)}$$

with

$$A_0(\mathbf{q}^2) \equiv \frac{1}{Z_\mu\mathbf{q}^2+R_\mu(\mathbf{q}^2)+\tilde{r}_\mu} \quad \text{(B9)}$$

and

$$\omega^{i_1i_2\ldots i_\ell}_{\mathcal{X}_1,\mathcal{X}_2,\ldots,\mathcal{X}_\ell} \equiv \sum_{i_{\ell+1},\ldots,i_{2\ell}=1}^{\frac{n(n-3)}{2}}T^{i_1i_2i_\ell i_{\ell+1}}_{\mathcal{X}_1}T^{i_2i_{\ell+1}i_{\ell+1}i_{\ell+2}}_{\mathcal{X}_2}\cdots T^{i_\ell i_{2\ell-1}i_{2\ell}}_{\mathcal{X}_\ell}. \quad \text{(B10)}$$

Plugging in homogeneous field configurations then yields dimensionless secondary couplings

$$V^{i_1i_2\ldots i_\ell}_{(\ell)*} \equiv Z_\mu^{-\frac{\ell}{2}}\mu^{\frac{d(\ell-2)}{2}-\ell}\left(\frac{K_d}{c_d}\right)^{\frac{(\ell-2)}{2}}\tilde{V}^{i_1i_2\ldots i_\ell}_{(\ell)*}, \quad \text{(B11)}$$

which we express in terms of the dimensionless independent couplings

$$r \equiv Z_\mu^{-1}\mu^{-2}\tilde{r}_\mu, \tag{B12}$$

$$g^{\mathcal{X}} \equiv Z_\mu^{-\frac{3}{2}}\mu^{\frac{d-6}{2}}\sqrt{\frac{K_d}{c_d}}\tilde{g}_\mu^{\mathcal{X}} \tag{B13}$$

with

$$K_d \equiv \frac{\mathrm{vol}(S^{d-1})}{(2\pi)^d} = \frac{1}{2^{d-1}\pi^{\frac{d}{2}}\Gamma\left(\frac{d}{2}\right)}. \tag{B14}$$

We shall later set the normalization constant, c_d, such that the final renormalization-group equations agree with the perturbative equations when expanded to one-loop order. Letting $(i_1 i_2 \ldots i_\ell)$ denote the symmetric average over $\ell!$ permutations of indices, we obtain

$$V_{(4)*}^{i_1 i_2 i_3 i_4} = -3s_3(r)\sum_{\mathcal{X}_1,\ldots,\mathcal{X}_4\in\{\mathrm{I},\mathrm{II}\}}\omega_{\mathcal{X}_1,\mathcal{X}_2,\mathcal{X}_3,\mathcal{X}_4}^{(i_1 i_2 i_3 i_4)}g^{\mathcal{X}_1}g^{\mathcal{X}_2}g^{\mathcal{X}_3}g^{\mathcal{X}_4}, \tag{B15}$$

$$V_{(5)*}^{i_1 i_2 i_3 i_4 i_5} = 12s_4(r)\sum_{\mathcal{X}_1,\ldots,\mathcal{X}_5\in\{\mathrm{I},\mathrm{II}\}}\omega_{\mathcal{X}_1,\mathcal{X}_2,\mathcal{X}_3,\mathcal{X}_4,\mathcal{X}_5}^{(i_1 i_2 i_3 i_4 i_5)}g^{\mathcal{X}_1}g^{\mathcal{X}_2}g^{\mathcal{X}_3}g^{\mathcal{X}_4}g^{\mathcal{X}_5}, \tag{B16}$$

where we have introduced the functions

$$s_\ell(r) \equiv \frac{c_d}{2}\int_0^\infty dy y^{\frac{d}{2}-1}\frac{1}{\{y+b(y)+r\}^{\ell+1}}, \tag{B17}$$

with

$$b(y) \equiv \frac{1}{Z_\mu\mu^2}R_\mu(\mathbf{q}^2=\mu^2 y). \tag{B18}$$

To evaluate the right-hand side of the Wetterich Eq. (B2), we need to invert the matrix

$$\left\{\Gamma_\mu^{(2)}[\phi]+R_\mu\mathbb{1}\right\}_{i,j}(\mathbf{q},\mathbf{q}') \tag{B19}$$

to cubic order in ϕ and evaluate diagonal elements. Along with the identity $\sum_{i=1}^{\frac{n(n-3)}{2}}T_{\mathcal{X}}^{iij}=0$, the following combinatorial relations prove useful in performing the algebra:

$$\sum_{i_3=1}^{\frac{n(n-3)}{2}}\sum_{\mathcal{X}_1,\mathcal{X}_2,\mathcal{X}_3,\mathcal{X}_4\in\{\mathrm{I},\mathrm{II}\}}g^{\mathcal{X}_1}g^{\mathcal{X}_2}g^{\mathcal{X}_3}g^{\mathcal{X}_4}\omega_{\mathcal{X}_1,\mathcal{X}_2,\mathcal{X}_3,\mathcal{X}_4}^{(i_1 i_2 i_3 i_3)} = \delta^{i_1 i_2}\left(\frac{2}{3}I_2^2+\frac{1}{3}I_4\right), \tag{B20}$$

$$\sum_{i_4,i_5=1}^{\frac{n(n-3)}{2}}\sum_{\mathcal{X}_1,\mathcal{X}_2,\mathcal{X}_3,\mathcal{X}_4,\mathcal{X}_5\in\{\mathrm{I},\mathrm{II}\}}g^{\mathcal{X}_1}g^{\mathcal{X}_2}g^{\mathcal{X}_3}g^{\mathcal{X}_4}g^{\mathcal{X}_5}\omega_{\mathcal{X}_1,\mathcal{X}_2,\mathcal{X}_3,\mathcal{X}_4}^{(i_1 i_2 i_4 i_5)}T_{\mathcal{X}_5}^{i_3 i_4 i_5} = \sum_{\mathcal{X}\in\{\mathrm{I},\mathrm{II}\}}T_{\mathcal{X}}^{i_1 i_2 i_3}\left(\frac{1}{3}I_{5,A}^{\mathcal{X}}+\frac{2}{3}I_{5,B}^{\mathcal{X}}\right), \tag{B21}$$

$$\sum_{i_4=1}^{\frac{n(n-3)}{2}}\sum_{\mathcal{X}_1,\mathcal{X}_2,\mathcal{X}_3,\mathcal{X}_4,\mathcal{X}_5\in\{\mathrm{I},\mathrm{II}\}}g^{\mathcal{X}_1}g^{\mathcal{X}_2}g^{\mathcal{X}_3}g^{\mathcal{X}_4}g^{\mathcal{X}_5}\omega_{\mathcal{X}_1,\mathcal{X}_2,\mathcal{X}_3,\mathcal{X}_4,\mathcal{X}_5}^{(i_1 i_2 i_3 i_4 i_4)} = \sum_{\mathcal{X}\in\{\mathrm{I},\mathrm{II}\}}T_{\mathcal{X}}^{i_1 i_2 i_3}\left(\frac{1}{2}I_2 I_3^{\mathcal{X}}+\frac{1}{2}I_{5,B}^{\mathcal{X}}\right), \tag{B22}$$

all of which can be derived by contracting indices of appropriate tensor products. We further define threshold functions

$$f_\ell(r) \equiv \frac{\ell c_d}{2}\int_0^\infty dy y^{\frac{d}{2}-1}\frac{c(y)}{\{y+b(y)+r\}^{\ell+1}}, \tag{B23}$$

$$m_1(r) \equiv c_d\int_0^\infty dy y^{\frac{d}{2}-1}c(y)\left[\frac{1+b'(y)+\frac{2y}{d}b''(y)}{\{y+b(y)+r\}^4} - \frac{4y}{d}\frac{\{1+b'(y)\}^2}{\{y+b(y)+r\}^5}\right], \tag{B24}$$

with

$$c(y) \equiv \frac{1}{Z_\mu\mu^2}\left(\mu\frac{\partial R_\mu}{\partial\mu}\right)(\mathbf{q}^2=\mu^2 y). \tag{B25}$$

Noting that the anomalous exponent is given by

$$\eta = -\mu\frac{\partial\log(Z_\mu)}{\partial\mu}, \tag{B26}$$

the resulting nonperturbative RG equations can be written as

$$\eta = \frac{1}{2}m_1(r)I_2(g), \tag{B27}$$

$$\beta_r \equiv \mu\frac{\partial r}{\partial\mu} = (-2+\eta)r+\frac{1}{2}f_2(r)I_2(g)+\{f_1(r)s_3(r)\}I_2^2(g) + \left\{\frac{1}{2}f_1(r)s_3(r)\right\}I_4(g), \tag{B28}$$

$$\beta^{\mathcal{X}} \equiv \mu\frac{\partial g^{\mathcal{X}}}{\partial\mu} = \left(\frac{d-6+3\eta}{2}\right)g^{\mathcal{X}}-f_3(r)I_3^{\mathcal{X}}(g) - \{3f_1(r)s_4(r)\}I_2(g)I_3^{\mathcal{X}}(g)-\left\{\frac{3}{2}f_2(r)s_3(r)\right\}I_{5,A}^{\mathcal{X}}(g) - \{3f_2(r)s_3(r)+3f_1(r)s_4(r)\}I_{5,B}^{\mathcal{X}}(g). \tag{B29}$$

To numerically study these equations, we selected the cutoff function

$$R_\mu(\mathbf{q}^2) = Z_\mu(\mu^2-\mathbf{q}^2)\theta(\mu^2-\mathbf{q}^2) \tag{B30}$$

and the normalization constant

$$c_d = \frac{d}{6}, \tag{B31}$$

which give

$$f_\ell(r) = \frac{\ell}{3(1+r)^{\ell+1}}\left(1-\frac{\eta}{d+2}\right), \tag{B32}$$

$$m_1(r) = \frac{1}{3(1+r)^4}, \tag{B33}$$

$$s_\ell(r) = \frac{1}{6(1+r)^{\ell+1}}+\frac{d}{6(2\ell+2-d)}\,{}_2F_1\left(\ell+1,\ell+1-\frac{d}{2};\ell+2-\frac{d}{2};-r\right), \tag{B34}$$

where we used

$$\int_0^\infty dy\theta(1-y)\delta(1-y) = \frac{1}{2}, \tag{B35}$$

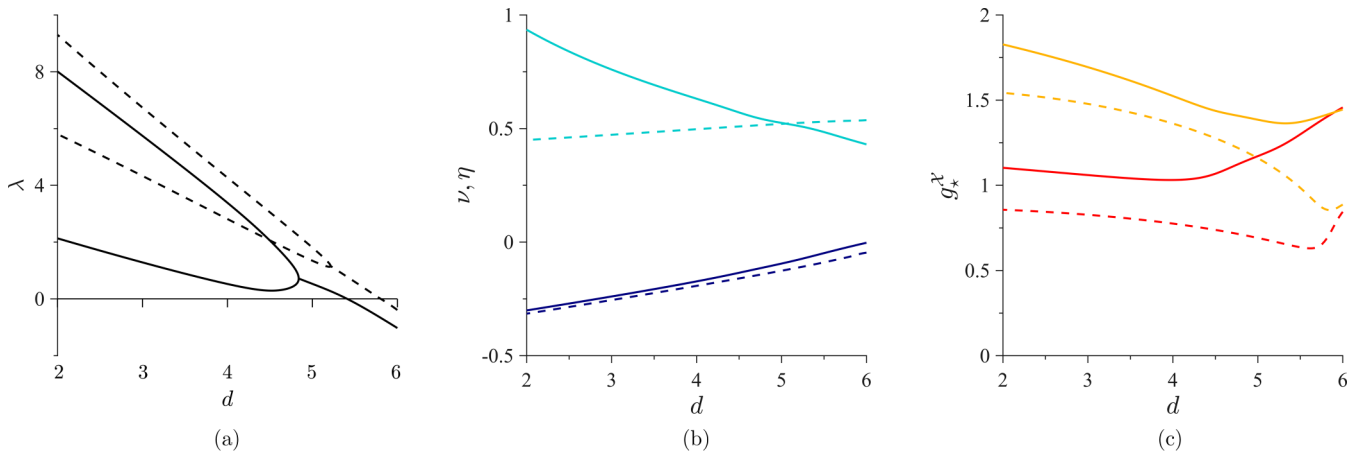

FIG. 4. Critical parameters at the nontrivial fixed point derived within the minimal two-loop (solid lines) and nonperturbative (dashed lines) RG schemes as functions of the spatial dimensions d. (a) Real parts of the stability exponents around the fixed point within the critical surface, λ_1 and λ_2. (b) Critical exponents, ν (cyan) and η (navy-blue). (c) Fixed-point values of running couplings, g^{I} (red) and g^{II} (orange) are of order unity in all d. Note that within the two-loop (nonperturbative) RG scheme, the nature of the fixed point changes at $d_0 \approx 4.8$ (5.2) and $d_{\mathrm{H}} \approx 5.4$ (5.8). Namely, two stability exponents merge for $d > d_0$, at which point they acquire imaginary parts. The flow thus spirals into the fixed point, but remains stable. Right above $d = d_{\mathrm{H}}$, the real part of these eigenvalues becomes negative and the flow spirals out of the fixed point to the limit cycle.

and ${}_2F_1$ is the ordinary hypergeometric function. Note that in general there can be some subtleties in dealing with products of step and δ functions [63], but within our approximation such subtleties do not arise.

Within this nonperturbative approach, unlike the perturbative dimensional regularization scheme, there is no clean way to focus on the critical surface from the onset. The analysis must instead include the quadratic coupling, $r(\mu)$, which essentially corresponds to the relevant deformation of the system away from the critical point. The RG flow is thus governed by three β functions, $\{\beta_r, \beta^{\mathrm{I}}, \beta^{\mathrm{II}}\}$, and the critical surface is defined by the global condition that a flow starting at $\{r, g^{\mathrm{I}}, g^{\mathrm{II}}\}$ must be attracted to the critical fixed point (or the critical limit cycle). In other words, a codimension-one hypersurface, $r_{\mathrm{c}}(g^{\mathrm{I}}, g^{\mathrm{II}})$, is identified over the range of $(g^{\mathrm{I}}, g^{\mathrm{II}})$ that can be made critical by tuning r, as long as the fixed point (or the cycle) remains critical with a single relevant deformation. Unfortunately the numerical analysis of the limit cycle then becomes overly arduous due to the need to tune out manually one relevant deformation. The stability exponents of the fixed point can nonetheless be obtained from the right eigenvalues of a 3×3 matrix

$$\left[\begin{array}{ccc} \frac{\partial\beta_r}{\partial r} & \frac{\partial\beta_r}{\partial g^{\mathrm{I}}} & \frac{\partial\beta_r}{\partial g^{\mathrm{II}}} \\ \frac{\partial\beta^{\mathrm{I}}}{\partial r} & \frac{\partial\beta^{\mathrm{I}}}{\partial g^{\mathrm{I}}} & \frac{\partial\beta^{\mathrm{I}}}{\partial g^{\mathrm{II}}} \\ \frac{\partial\beta^{\mathrm{II}}}{\partial r} & \frac{\partial\beta^{\mathrm{II}}}{\partial g^{\mathrm{I}}} & \frac{\partial\beta^{\mathrm{II}}}{\partial g^{\mathrm{II}}} \end{array}\right]\Bigg|_{(r,g^{\mathrm{I}},g^{\mathrm{II}})=(r_\star,g^{\mathrm{I}}_\star,g^{\mathrm{II}}_\star)}, \tag{B36}$$

with the lowest value, λ_0, yielding the critical exponent, $\nu = -1/\lambda_0$, while λ_1 and λ_2 again control subleading corrections near the critical point. The results in Fig. 4 qualitatively agree with the minimal two-loop RG treatment and thus bring additional support to the existence of the nontrivial critical fixed point. Quantitatively, however, they do not completely match. Most notably the exponent ν displays an opposite trend with d. This discrepancy may be stemming from simplifications related to our present inability to properly treat Nambu-Goldstone soft modes around the RSB phase.

[1] P. W. Anderson, Absence of diffusion in certain random lattices, Phys. Rev. **109**, 1492 (1958).

[2] D. M. Basko, I. L. Aleiner, and B. L. Altshuler, Metal–insulator transition in a weakly interacting many-electron system with localized single-particle states, Ann. Phys. **321**, 1126 (2006).

[3] V. Oganesyan and D. A. Huse, Localization of interacting fermions at high temperature, Phys. Rev. B **75**, 155111 (2007).

[4] A. Pal and D. A. Huse, Many-body localization phase transition, Phys. Rev. B **82**, 174411 (2010).

[5] N. F. Mott, Conduction in non-crystalline materials: III. Localized states in a pseudogap and near extremities of conduction and valence bands, Philos. Mag. **19**, 835 (1969).

[6] V. Ambegaokar, B. I. Halperin, and J. S. Langer, Hopping conductivity in disordered systems, Phys. Rev. B **4**, 2612 (1971).

[7] A. L. Efros and B. I. Shklovskii, Coulomb gap and low temperature conductivity of disordered systems, J. Phys. C **8**, L49 (1975).

[8] Y. Imry and S.-K. Ma, Random-Field Instability of the Ordered State of Continuous Symmetry, Phys. Rev. Lett. **35**, 1399 (1975).

[9] G. Parisi, Infinite Number of Order Parameters for Spin-Glasses, Phys. Rev. Lett. **43**, 1754 (1979).

[10] M. Mézard, G. Parisi, and M. Virasoro, *Spin Glass Theory and Beyond* (World Scientific, Singapore, 1987).

[11] S. F. Edwards and P. W. Anderson, Theory of spin glasses, J. Phys. F: Metal Phys. **5**, 965 (1975).

[12] S. Kirkpatrick and D. Sherrington, Infinite-ranged models of spin-glasses, Phys. Rev. B **17**, 4384 (1978).

[13] J. R. L. de Almeida and D. J. Thouless, Stability of the Sherrington-Kirkpatrick solution of a spin glass model, J. Phys. A: Math. Gen. **11**, 983 (1978).

[14] F. Guerra, Broken replica symmetry bounds in the mean field spin glass model, Commun. Math. Phys. **233**, 1 (2003).

[15] M. Talagrand, The Parisi formula, Ann. Math. **163**, 221 (2006).

[16] E. Gardner, Spin glasses with p-spin interactions, Nucl. Phys. B **257**, 747 (1985).

[17] D. J. Gross, I. Kanter, and H. Sompolinsky, Mean-Field Theory of the Potts Glass, Phys. Rev. Lett. **55**, 304 (1985).

[18] P. Charbonneau, J. Kurchan, G. Parisi, P. Urbani, and F. Zamponi, Fractal free energy landscapes in structural glasses, Nat. Commun. **5**, 3725 (2014).

[19] C. M. Newman and D. L. Stein, Ordering and broken symmetry in short-ranged spin glasses, J. Phys.: Condens. Matter **15**, R1319 (2003).

[20] W. L. McMillan, Scaling theory of Ising spin glasses, J. Phys. C: Solid State Phys. **17**, 3179 (1984).

[21] A. J. Bray and M. A. Moore, Critical behavior of the three-dimensional Ising spin glass, Phys. Rev. B **31**, 631 (1985).

[22] D. S. Fisher and D. A. Huse, Ordered Phase of Short-Range Ising Spin-Glasses, Phys. Rev. Lett. **56**, 1601 (1986).

[23] D. A. Huse and D. S. Fisher, Pure states in spin glasses, J. Phys. A: Math. Gen. **20**, L997 (1987).

[24] A. J. Bray and M. A. Moore, Scaling theory of the ordered phase of spin glasses, in *Heidelberg Colloquium on Glassy Dynamics: Proceedings of a Colloquium on Spin Glasses, Optimization and Neural Networks Held at the University of Heidelberg, June 9–13, 1986*, edited by J. L. van Hemmen and I. Morgenstern (Springer, Berlin/Heidelberg, 1987), p. 121.

[25] D. S. Fisher and D. A. Huse, Equilibrium behavior of the spin-glass ordered phase, Phys. Rev. B **38**, 386 (1988).

[26] O. L. White and D. S. Fisher, Scenario for Spin-Glass Phase with Infinitely Many States, Phys. Rev. Lett. **96**, 137204 (2006).

[27] M. A. Moore and A. J. Bray, Disappearance of the de Almeida-Thouless line in six dimensions, Phys. Rev. B **83**, 224408 (2011).

[28] G. Parisi and T. Temesvári, Replica symmetry breaking in and around six dimensions, Nucl. Phys. B **858**, 293 (2012).

[29] T. Temesvári, Comment on Critical point scaling of Ising spin glasses in a magnetic field, Phys. Rev. B **94**, 176401 (2016).

[30] T. Temesvári, Physical observables of the Ising spin glass in 6-ε dimensions: Asymptotical behavior around the critical fixed point, Phys. Rev. B **96**, 024411 (2017).

[31] A. J. Bray and S. A. Roberts, Renormalization-group approach to the spin glass transition in finite magnetic fields, J. Phys. C: Solid State Phys. **13**, 5405 (1980).

[32] I. R. Pimentel, T. Temesvari, and C. De Dominicis, Spin glass transition in a magnetic field: A renormalization group study, Phys. Rev. B **65**, 224420 (2002).

[33] P. Urbani and G. Biroli, Gardner transition in finite dimensions, Phys. Rev. B **91**, 100202(R) (2015).

[34] M. C. Angelini and G. Biroli, Spin Glass in a Field: A New Zero-Temperature Fixed Point in Finite Dimensions, Phys. Rev. Lett. **114**, 095701 (2015).

[35] C. Rainone, P. Urbani, H. Yoshino, and F. Zamponi, Following the Evolution of Hard Sphere Glasses in Infinite Dimensions under External Perturbations: Compression and Shear Strain, Phys. Rev. Lett. **114**, 015701 (2015).

[36] G. Biroli and P. Urbani, Breakdown of elasticity in amorphous solids, Nat. Phys. **12**, 1130 (2016).

[37] M. C. Angelini and G. Biroli, Real space renormalization group theory of disordered models of glasses, Proc. Natl. Acad. Sci. USA **114**, 3328 (2017).

[38] Y. Jin and H. Yoshino, Exploring the complex free-energy landscape of the simplest glass by rheology, Nat. Commun. **8**, 14935 (2017).

[39] P. Charbonneau and S. Yaida, Nontrivial Critical Fixed Point for Replica-Symmetry-Breaking Transitions, Phys. Rev. Lett. **118**, 215701 (2017).

[40] W. E. Caswell, Asymptotic Behavior of Non-Abelian Gauge Theories to Two-Loop Order, Phys. Rev. Lett. **33**, 244 (1974).

[41] T. Banks and A. Zaks, On the phase structure of vector-like gauge theories with massless fermions, Nucl. Phys. B **196**, 189 (1982).

[42] G. A. Baker, Jr., B. G. Nickel, M. S. Green, and D. I. Meiron, Ising-Model Critical Indices in Three Dimensions from the Callan-Symanzik Equation, Phys. Rev. Lett. **36**, 1351 (1976).

[43] M. B. Weissman, What is a spin glass? A glimpse via mesoscopic noise, Rev. Mod. Phys. **65**, 829 (1993).

[44] J. A. Mydosh, *Spin Glasses: An Experimental Introduction* (CRC Press, Boca Raton, 2014).

[45] A. Seguin and O. Dauchot, Experimental Evidence of the Gardner Phase in a Granular Glass, Phys. Rev. Lett. **117**, 228001 (2016).

[46] K. Geirhos, P. Lunkenheimer, and A. Loidl, Johari-Goldstein Relaxation Far Below T_g: Experimental Evidence for the Gardner Transition in Structural Glasses? Phys. Rev. Lett. **120**, 085705 (2018).

[47] R. A. Baños, A. Cruz, L. A. Fernandez, J. M. Gil-Narvion, A. Gordillo-Guerrero, M. Guidetti, D. Iñiguez, A. Maiorano, E. Marinari, V. Martin-Mayor, J. Monforte-Garcia, A. Muñoz Sudupe, D. Navarro, G. Parisi, S. Perez-Gaviro, J. J. Ruiz-Lorenzo, S. F. Schifano, B. Seoane, A. Tarancon, P. Tellez, R. Tripiccione, and D. Yllanes, Thermodynamic glass transition in a spin glass without time-reversal symmetry, Proc. Natl. Acad. Sci. USA **109**, 6452 (2012).

[48] M. Baity-Jesi, R. A. Baños, A. Cruz, L. A. Fernandez, J. M. Gil-Narvion, A. Gordillo-Guerrero, D. Iñiguez, A. Maiorano, F. Mantovani, E. Marinari, V. Martin-Mayor, J. Monforte-Garcia, A. Muñoz Sudupe, D. Navarro, G. Parisi, S. Perez-Gaviro, M. Pivanti, F. Ricci-Tersenghi, J. J. Ruiz-Lorenzo, S. F. Schifano, B. Seoane, A. Tarancon, R. Tripiccione, and D. Yllanes, Dynamical transition in the $d = 3$ Edwards-Anderson spin glass in an external magnetic field, Phys. Rev. E **89**, 032140 (2014).

[49] L. Berthier, P. Charbonneau, Y. Jin, G. Parisi, B. Seoane, and F. Zamponi, Growing timescales and lengthscales characterizing vibrations of amorphous solids, Proc. Natl. Acad. Sci. USA **113**, 8397 (2016).

[50] C. Scalliet, L. Berthier, and F. Zamponi, Absence of Marginal Stability in a Structural Glass, Phys. Rev. Lett. **119**, 205501 (2017).

[51] P. Charbonneau, E. I. Corwin, L. Fu, G. Tsekenis, and M. van der Naald, Glassy, Gardner-like phenomenology in minimally polydisperse crystalline systems, Phys. Rev. E **99**, 020901(R) (2019).

[52] B. Seoane and F. Zamponi, Spin-glass–like aging in colloidal and granular glasses, Soft Matter **14**, 5222 (2018).

[53] D. Stauffer and A. Aharony, *Introduction to Percolation Theory*, revised 2nd ed. (CRC Press, Boca Raton, 2014).
[54] D. Ben-Avraham and S. Havlin, *Diffusion and Reactions in Fractals and Disordered Systems* (Cambridge University Press, Cambridge, 2000).
[55] B. Charbonneau, P. Charbonneau, and G. Tarjus, Geometrical frustration and static correlations in hard-sphere glass formers, J. Chem. Phys. **138**, 12A515 (2013).
[56] P. Charbonneau, J. Kurchan, G. Parisi, P. Urbani, and F. Zamponi, Glass and jamming transitions: From exact results to finite-dimensional descriptions, Annu. Rev. Condens. Matter Phys. **8**, 265 (2017).
[57] N. Goldenfeld, *Lectures on Phase Transitions and the Renormalization Group* (CRC Press, Boca Raton, 2018).
[58] J. A. Gracey, Four loop renormalization of ϕ^3 theory in six dimensions, Phys. Rev. D **92**, 025012 (2015).
[59] J. Zinn-Justin, Summation of divergent series: Order-dependent mapping, Appl. Num. Math. **60**, 1454 (2010).
[60] G. V. Dunne and M. Ünsal, What is QFT? Resurgent trans-series, Lefschetz thimbles, and new exact saddles, PoS (LATTICE 2015) **251**, 010 (2016).
[61] J. Polchinski, Renormalization and effective Lagrangians, Nucl. Phys. B **231**, 269 (1984).
[62] C. Wetterich, Exact evolution equation for the effective potential, Phys. Lett. B **301**, 90 (1993).
[63] T. R. Morris, The exact renormalization group and approximate solutions, Int. J. Mod. Phys. A **9**, 2411 (1994).
[64] J. Berges, N. Tetradis, and C. Wetterich, Nonperturbative renormalization flow in quantum field theory and statistical physics, Phys. Rep. **363**, 223 (2002).
[65] G. Tarjus and M. Tissier, Nonperturbative Functional Renormalization Group for Random Field Models: The Way Out of Dimensional Reduction, Phys. Rev. Lett. **93**, 267008 (2004).
[66] B. Delamotte, An introduction to the nonperturbative renormalization group, Lect. Notes Phys. **852**, 49 (2012).
[67] R. Rattazzi, V. S. Rychkov, E. Tonni, and A. Vichi, Bounding scalar operator dimensions in 4D CFT, J. High Energy Phys. 12 (2008) 031.
[68] S. El-Showk, M. F. Paulos, D. Poland, S. Rychkov, D. Simmons-Duffin, and A. Vichi, Solving the 3D ising model with the conformal bootstrap, Phys. Rev. D **86**, 025022 (2012).
[69] F. Gliozzi, Constraints on Conformal Field Theories in Diverse Dimensions from the Bootstrap Mechanism, Phys. Rev. Lett. **111**, 161602 (2013).
[70] S. El-Showk, M. F. Paulos, D. Poland, S. Rychkov, D. Simmons-Duffin, and A. Vichi, Solving the 3d Ising model with the conformal bootstrap. II. c-minimization and precise critical exponents, J. Stat. Phys. **157**, 869 (2014).
[71] M. A. Moore and N. Read, Multicritical Point on the de Almeida-Thouless Line in Spin Glasses in $d > 6$ Dimensions, Phys. Rev. Lett. **120**, 130602 (2018).
[72] We used the fourth-order Runge-Kutta integration with timestep $dt \equiv d\mu/\mu = 10^{-5}$.
[73] D. Sornette, A. Johansen, and J.-P. Bouchaud, Stock market crashes, precursors and replicas, J. Phys. I France **6**, 167 (1996).
[74] D. Sornette, Discrete-scale invariance and complex dimensions, Phys. Rep. **297**, 239 (1998).
[75] G. V. Dunne, Heisenberg–Euler effective Lagrangians: Basics and extensions, in *From Fields to Strings: Circumnavigating Theoretical Physics: Ian Kogan Memorial Collection (In 3 Volumes)* (World Scientific, Singapore, 2005), p. 445.
[76] A. Raju, C. B. Clement, L. X. Hayden, J. P. Kent-Dobias, D. B. Liarte, D. Rocklin, and J. P. Sethna, Renormalization group and normal form theory, arXiv:1706.00137.
[77] P. Charbonneau, Y. Hu, A. Raju, J. Sethna, and S. Yaida, Data and scripts from: Morphology of renormalization-group flow for the de Almeida—Thouless—Gardner universality class (2019), Duke Digital Repository at https://doi.org/10.7924/r4zc7wm7d
[78] C. Bervillier, Exact renormalization group equation for the Lifshitz critical point, Phys. Lett. A **331**, 110 (2004).
[79] M. Tissier and G. Tarjus, Unified Picture of Ferromagnetism, Quasi-Long-Range Order and Criticality in Random-Field Models, Phys. Rev. Lett. **96**, 087202 (2006).
[80] M. Tissier and G. Tarjus, Supersymmetry and its Spontaneous Breaking in the Random Field Ising Model, Phys. Rev. Lett. **107**, 041601 (2011).
[81] L. Canet, B. Delamotte, and N. Wschebor, Fully developed isotropic turbulence: Nonperturbative renormalization group formalism and fixed-point solution, Phys. Rev. E **93**, 063101 (2016).
[82] A. Margaritis, G. Ódor, and A. Patkós, Series expansion solution of the Wegner-Houghton renormalisation group equation, Z. Phys. C **39**, 109 (1988).
[83] T. Papenbrock and C. Wetterich, Two loop results from one loop computations and nonperturbative solutions of exact evolution equations, Z. Phys. C **65**, 519 (1995).